DEVELOPMENTAL DYNAMICS 243:818–832, 2014
DOI: 10.1002/DVDY.24122

Temporal Regulation of Dpp Signaling Output in the *Drosophila* Wing

David D. O'Keefe,[1] Sean Thomas,[2] Bruce A. Edgar,[3] and Laura Buttitta[4]*

[1]Division of Basic Sciences, Fred Hutchinson Cancer Research Center, Seattle, Washington
[2]Gladstone Institute for Cardiovascular Disease, J David Gladstone Institutes, San Francisco, California
[3]German Cancer Research Center (DKFZ)-Center for Molecular Biology Heidelberg (ZMBH) Alliance, Im Neuenheimer Feld 282, Heidelberg, Germany
[4]Molecular Cellular and Developmental Biology, University of Michigan, Ann Arbor, Michigan

Background: The Decapentaplegic (Dpp) signaling pathway is used in many developmental and homeostatic contexts, each time resulting in cellular responses particular to that biological niche. The flexibility of Dpp signaling is clearly evident in epithelial cells of the *Drosophila* wing imaginal disc. During larval stages of development, Dpp functions as a morphogen, patterning the wing developmental field and stimulating tissue growth. A short time later, however, as wing-epithelial cells exit the cell cycle and begin to differentiate, Dpp is a critical determinant of vein-cell fate. It is likely that the Dpp signaling pathway regulates different sets of target genes at these two developmental time points. Results: To identify mechanisms that temporally control the transcriptional output of Dpp signaling in this system, we have taken a gene expression profiling approach. We identified genes affected by Dpp signaling at late larval or early pupal developmental time points, thereby identifying patterning- and differentiation-specific downstream targets, respectively. Conclusions: Analysis of target genes and transcription factor binding sites associated with these groups of genes revealed potential mechanisms by which target-gene specificity of the Dpp signaling pathway is temporally regulated. In addition, this approach revealed novel mechanisms by which Dpp affects the cellular differentiation of wing-veins. *Developmental Dynamics 243:818–832, 2014*. © 2014 Wiley Periodicals, Inc.

Key words: wing; epithelium; imaginal disc; *decapentaplegic*; *thickveins*; metamorphosis

Submitted 22 August 2013; First Decision 25 February 2014; Accepted 25 February 2014; Published online 2 March 2014

Introduction

Intercellular signaling pathways translate environmental cues into transcriptional responses that alter a wide range of cellular properties. Each signaling pathway, however, is typically utilized in many developmental and homeostatic contexts, suggesting that the transcriptional outputs of signaling events are both spatially and temporally regulated. Although this idea has been appreciated for decades (reviewed by Barolo and Posakony, 2002), mechanisms that customize target-gene specificity to a particular biological niche have not been adequately described.

The Decapentaplegic (Dpp) signaling pathway in *Drosophila* participates in many biological processes, as the name implies (Spencer et al., 1982). Dpp specifies cell fates along the dorsal/ventral axis of the early embryo (Irish and Gelbart, 1987), regulates cell shape and migration during dorsal closure (Hou et al., 1997; Riesgo-Escovar and Hafen, 1997; Fernandez et al., 2007), and maintains stem-cell homeostasis (Xie and Spradling, 1998; Li et al., 2013), to name just a few of its functions. Dpp has been studied most intensely, however, within the developing wing epithelium. During larval stages of development, Dpp functions as a morphogen, stimulating cell growth and proliferation and specifying positional identity in a concentration-dependent manner (reviewed in Wartlick et al., 2011a). Many factors regulate the shape of the Dpp morphogen gradient (i.e., affect its diffusion across the wing epithelium), but it is less clear how different concentrations of Dpp are translated into different transcriptional responses (Affolter and Basler, 2007). It is also unclear how the functional readout of Dpp signaling shifts dramatically after pupariation. As wing epithelial cells exit the cell cycle and begin to differentiate, Dpp no longer functions as a morphogen, but instead becomes a critical determinant of vein cell fate (Sotillos and de Celis, 2006). It is likely, therefore, that Dpp signaling regulates different sets of target genes at larval and pupal stages of development. As such, the *Drosophila* wing provides a unique opportunity to study how the transcriptional output of a signaling pathway is temporally regulated within a single tissue.

Binding of Dpp to its receptors, Punt and Thickvein (Tkv), results in the phosporylation of Mothers against Dpp (Mad) and translocation of phosporylated Mad (pMad), along with the co-

Grant sponsor: NIH; Grant numbers: GM070887; GM086517; Grant sponsor: NCI; Grant number: 1 U54 CA132381.
*Correspondence to: Laura Buttitta, Molecular Cellular and Developmental Biology, University of Michigan, Ann Arbor, MI 48109. buttitta@umich.edu

Article is online at: http://onlinelibrary.wiley.com/doi/10.1002/dvdy.24122/abstract

Smad, Medea, into the nucleus (Das et al., 1998; Inoue et al., 1998). Once in the nucleus, the pMad/Medea complex interacts with cofactors such as Schnurri to activate, repress, or de-repress target genes (reviewed in Affolter and Basler, 2007). Regulatory sequences bound by pMad/Medea, therefore, play an important role in determining Dpp target-gene specificity. To alter output based on Dpp concentration, for example, pMad-binding sites differ in both affinity (Wharton et al., 2004) and spacing (Lin et al., 2006). In addition, pMad-mediated transcription can be affected by the proximity of other transcription-factor binding sites, which allows selector genes or other signaling pathways to affect the functional output of Dpp signaling (Liang et al., 2012; Nfonsam et al., 2012).

Here we have taken a gene-expression profiling approach to explore the temporal regulation of Dpp target-gene specificity in the *Drosophila* wing. We over-expressed an activated version of the Tkv receptor (Tkv^{Q235D}) in wing epithelial cells at late larval or early pupal developmental time points, identifying patterning- and differentiation-specific downstream targets, respectively. Binding-site analysis revealed potential mechanisms by which signaling targets are temporally regulated. In addition, this analysis provided insights into how Dpp affects wing-vein morphogenesis.

Results and Discussion

Temporal Specificity of the Dpp Signaling Pathway

The pattern of activity associated with the Dpp signaling pathway (i.e., pMad localization) changes dramatically during wing metamorphosis (Sotillos and de Celis, 2006). In the larval wing disc, pMad levels are highest medially, reflecting the well-studied gradient of Dpp (Fig. 1A). This pattern is maintained during early stages of wing metamorphosis, but between 6 and 18 hr APF, the pMad gradient is lost and pMad instead localizes to presumptive veins (Fig. 1B).

As a first step toward analyzing the temporal-specific effects of Dpp, we used a temperature-sensitive Gal4 system to activate Dpp signaling for very short periods of time. The *apterous-Gal4* (ap^{Gal4}) driver expresses Gal4 in dorsal cells of the L3 wing disc (Fig. 1C) and the pupal wing (Fig. 1D) (Calleja et al., 1996). When combined with a temperature-sensitive *tubulin-Gal80* transgene ($tubulin\text{-}Gal80^{ts}$) (McGuire et al., 2003), this driver can be temporally regulated. We call this the ap^{ts} system (genotype: ap^{Gal4},*UAS-GFP/CyO;tubulin-*$Gal80^{ts}$) and used it to express an activated version of the Dpp receptor, Tkv (Tkv^{Q235D}). When animals were raised at 18°C with no temperature shift, expression from the $UAS\text{-}Tkv^{Q235D}$ transgene was not induced, as levels of pMad were not affected (data not shown), and adult wings were wild type in appearance (Fig. 1I) (genotype: $hsflp^{112}$/+; ap^{Gal4},*UAS-GFP/+;tubulin-*$Gal80^{ts}$/$UAS\text{-}Tkv^{Q235D}$). We then performed 10-hr temperature shifts (18° to 30°C) immediately before dissecting wing tissue at either the late L3 developmental stage (wandering larvae) or 24 hr APF (an early pupal stage). These two developmental stages are separated by approximately 24–30 hr (at 25°C). In both cases, the level of pMad was dramatically elevated in dorsal, Tkv^{Q235D}-expressing cells, compared to ventral cells, which served as an internal control (Fig. 1E,F). As levels of pMad are normally the same in dorsal and ventral cells (Fig. 1A and data not shown), this indicated that Dpp signaling had been activated.

As a 10-hr temperature shift was sufficient to activate Dpp signaling, we repeated this protocol and analyzed effects on vein/intervein cell fate and cell proliferation. To assess cell fate, L3 wing discs and 24-hr APF pupal wings were stained for Blistered (Bs), which specifically labels intervein cells (Montagne et al., 1996). Importantly, levels of Bs are similar in dorsal and ventral cells of wild-type wing tissue (data not shown). When the temperature shift was performed during pupal stages (from 14–24 hr APF), Tkv^{Q235D} down-regulated Bs levels in dorsal cells of the wing compared to ventral cells (Fig. 1H). This agreed with the known role of Dpp in promoting vein-cell fate during pupal stages of development (de Celis, 1997). If these animals were returned to 18°C and allowed to develop into adults, numerous ectopic veins were observed (Fig. 1K). In contrast, Tkv^{Q235D} expression in dorsal cells during the late L3 stage did not affect Bs levels (Fig. 1G), and adult wings from these animals (if returned to 18°C) had normal patterns of venation (Fig. 1J). As such, Dpp's ability to affect vein/intervein cell fate was temporally regulated (i.e., acquired during early stages of pupal development).

Whereas expression of Tkv^{Q235D} during late L3 did not affect cell fate, resulting adult wings were generally curved (Fig. 1J). The downward wing curvature suggests a larger dorsal surface (Raisin et al., 2003), which is consistent with increased levels of tissue growth via Fat signaling in Tkv^{Q235D}-expressing cells (Rogulja et al., 2008). This curvature was most prominent laterally (i.e., near veins L2 and L5), which is also consistent with previously observed Dpp-induced ectopic proliferation (Martin-Castellanos and Edgar, 2002). In summary, using the ap^{ts} system to activate Dpp signaling in the wing resulted in different phenotypic outcomes depending on the developmental stage, suggesting that the set of target genes regulated by the Dpp signaling pathway changes within this tissue over a short period of time.

Targets of the Dpp Signaling Pathway

To compare larval and pupal sets of putative Dpp target genes, we performed a microarray analysis. The ap^{ts} system was used to express Tkv^{Q235D} along with GFP or GFP alone in dorsal cells of the wing for 10 hr, and RNA was collected from wing tissue at either late L3 or 24 hr APF. Potential L3 targets were identifying by comparing gene-expression profiles of discs expressing Tkv^{Q235D}/GFP to discs expressing GFP alone. Similarly, pupal-wing targets were identified by comparing wings expressing Tkv^{Q235D} /GFP to wings expressing GFP alone (Fig. 2A). This strategy yielded 624 genes whose expression was affected by Dpp signaling at one or both of these developmental time points within 10 hr (Fig. 2B,C). Many of these potential target genes were time-point specific (i.e., Tkv^{Q235D} altered their level of expression at one developmental time point but not the other). A small number of genes were even inversely regulated (e.g., up-regulated at L3 and down-regulated at 24 hr APF). We also noted that gene expression changes were roughly symmetric, meaning similar numbers of genes were up and down-regulated at each timepoint. Within wing tissue, therefore, the transition between larval and pupal stages of development coincides with a switch in the set of genes affected by Dpp signaling.

There are several limitations associated with using a microarray approach to analyze temporal changes in Dpp-signaling output. First, this approach will only identify changes in mRNA levels, which excludes known effects of Dpp signaling on

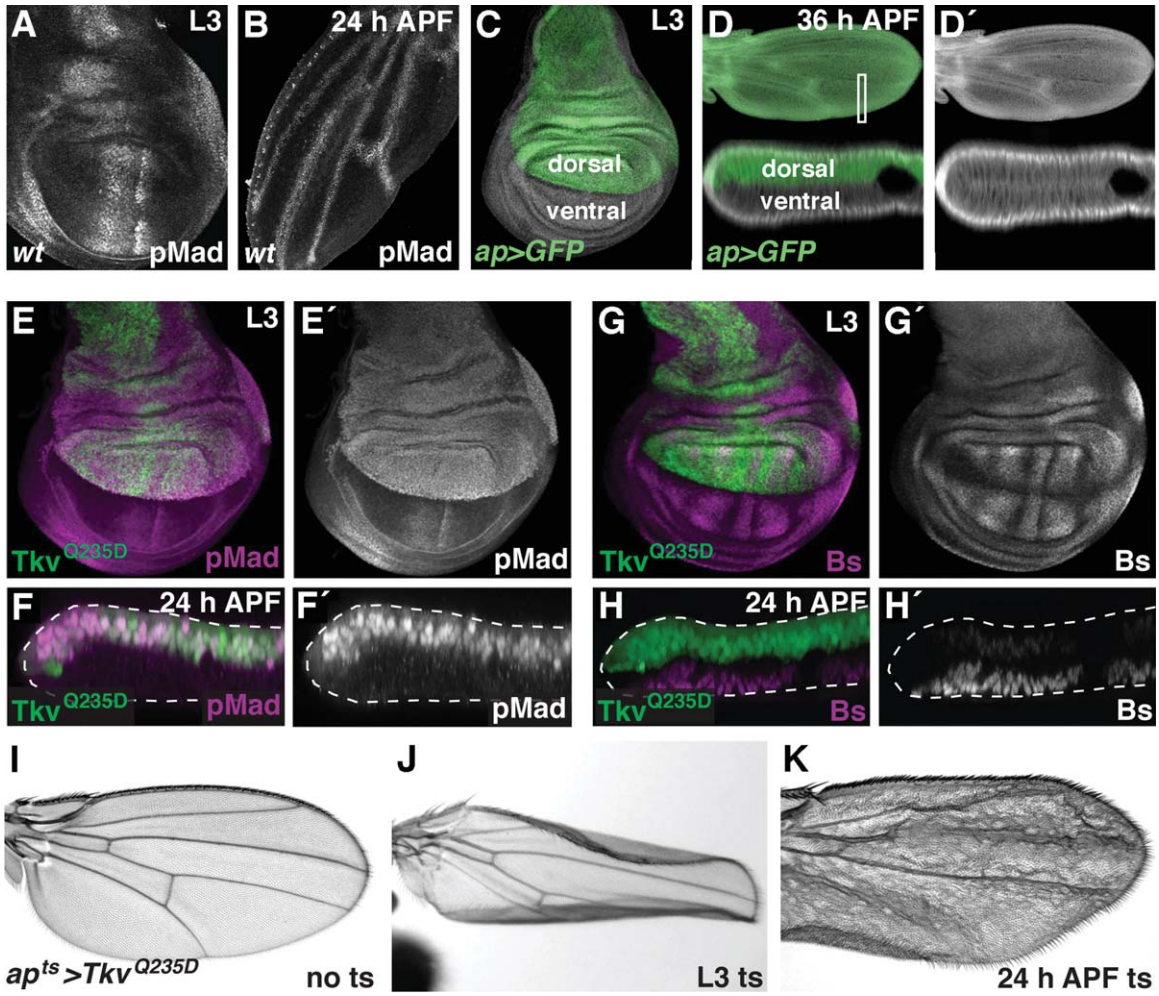

Fig. 1. Temporal-specific phenotypes associated with Dpp signaling in the wing. **A,B:** Wing tissue was dissected and stained for phosphorylated Mad (pMad), a readout of Dpp activity. Developmental stages are indicated. **C,D:** The ap^{Gal4} driver was used to express GFP in L3 wing discs (C) and pupal wings (D). Cells fated to give rise to dorsal and ventral cells of the wing are indicated. In D an optical cross-section through the posterior margin and the L4 wing vein (boxed region) is shown below. Tissues are labeled with Hoechst (C and D, top) or antibodies against Discs large 1 (D, below). **E–H, J, K:** The ap^{ts} system was used to express Tkv^{Q235D} (along with GFP) in dorsal wing cells at specific stages of development. Animals were temperature shifted for 10 hr during larval (E,G,J) or pupal (F,H,K) stages, and dissections performed at developmental time points indicated (late L3 or 24 hr APF). For pupal wing images (F and H), optical cross-sections are shown (similar to the boxed region in D). Using this protocol, levels of pMad were elevated in dorsal, Tkv^{Q235D}-expressing cells (compared to ventral cells, which serve as an internal control) at both larval (E) and pupal (F) stages. G, H: Bs localizes to intervein cells in both the dorsal and ventral wing. Tkv^{Q235D} did not affect Bs levels in dorsal cells of the larval wing disc compared to ventral cells (G), but down-regulated Bs in dorsal cells of the pupal wing (H). This indicated a temporal-specific effect of Dpp signaling. **I:** In the absence of a temperature shift, ap^{ts} Tkv^{Q235D} animals had phenotypically wild-type wings. J: Expression of Tkv^{Q235D} for 10 hr during late L3 resulted in a curved wing (expanded dorsal surface). K: Expression of Tkv^{Q235D} from 14–24-hr APF resulted in ectopic vein tissue. **D′,E′,F′,G′** and **H′** show single-channel excerpts of their respective images.

microRNAs (Oh and Irvine, 2011). Second, potential downstream targets may represent direct targets of Dpp signaling (through the transcription factor Mad), or they may represent targets of other signaling pathways affected by Dpp. These indirect targets may include, for example, changes in gene expression that result from altered Fat localization (Rogulja et al., 2008). Third, by expressing Tkv^{Q235D} for only 10 hr, we intend to enrich for direct Dpp targets, but our dataset may also include rapid indirect responses or possibly lack direct transcriptional responses that occur more slowly. Finally, because we are isolating mRNA from whole wings and the ap^{Gal4} driver activates Dpp signaling only in dorsal cells, effects on gene expression will be diluted by the necessary inclusion of unperturbed ventral cells.

Behavior of Known Dpp Targets After 10 Hr of Induction

We first examined expression changes for known targets of Dpp in the wing. Several direct targets, namely *Daughters against dpp* (*Dad*), *larval translucida* (*ltl*), *crossveinless 2* (*cv-2*), and *knirps* (*kni*) (Serpe et al., 2008; Weiss et al., 2010; Szuperak et al., 2011), displayed expected changes in gene expression, but only in the 24-hr APF pupal wing (Table 1). Other known targets, namely *brinker* (*brk*), *pentagone* (*pent*), *spalt* (*sal*), *optomotor-blind* (*omb*), and *vestigial* (*vg*) (Kim et al., 1997; Pyrowolakis et al., 2004; Vuilleumier et al., 2010) were not associated with a significant change in expression at either time point. We inspected the raw

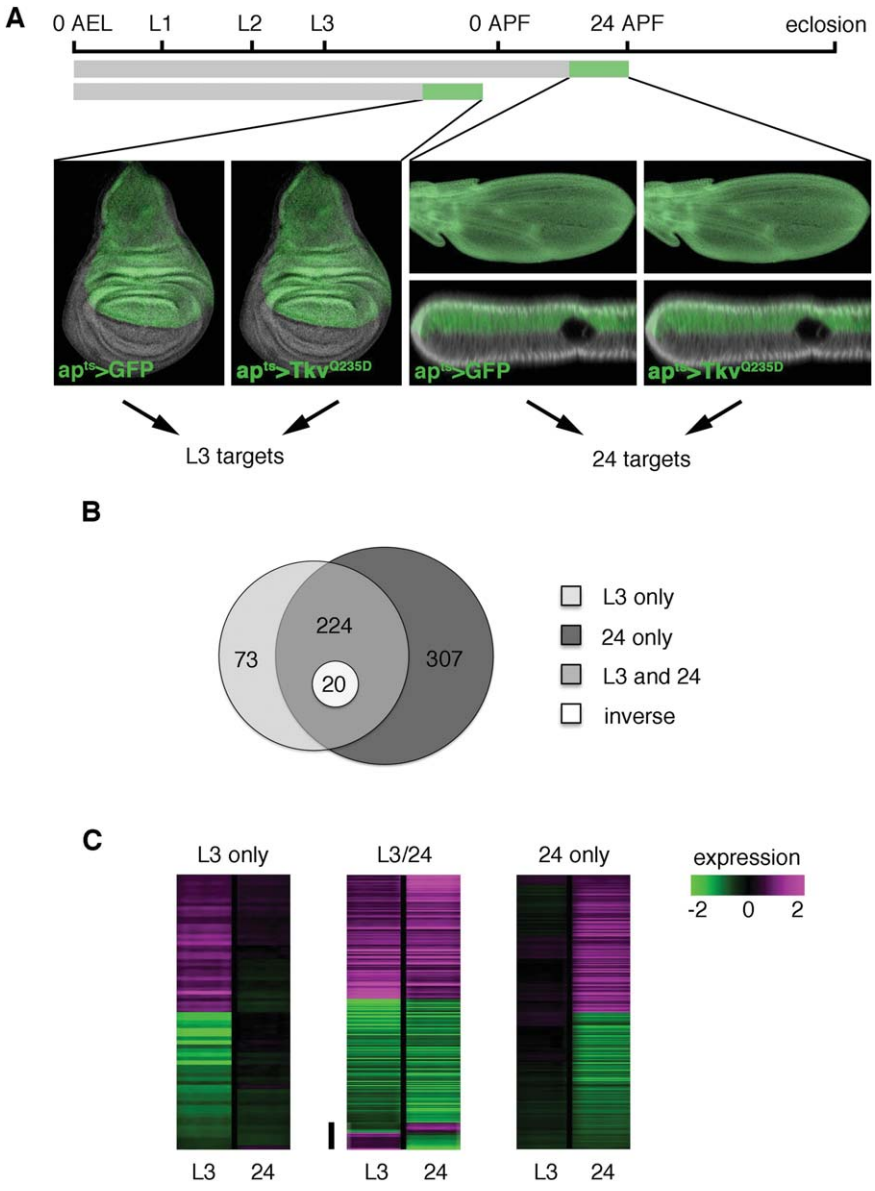

Fig. 2. Gene-expression changes in response to Dpp signaling. **A:** A schematic representation of the experimental system is shown. The ap^{ts} system was used to express either GFP or Tkv^{Q235D}/GFP for 10 hr in the developing wing before dissection. Tissue was dissected at late L3 (end of the larval stage) or 24 hr APF (early pupal stage). Microarray analysis was used to compare gene-expression profiles of discs expressing GFP to discs expressing Tkv^{Q235D}/GFP. Similarly, pupal wings expressing GFP were compared to pupal wings expressing Tkv^{Q235D}/GFP. In this way, Tkv^{Q235D}-responsive genes were determined for these two developmental time points. **B:** A Venn diagram indicates the numbers of genes affected by Dpp signaling at these developmental time points. **C:** Heat map representations of gene expression changes are shown for the four types of target genes: those regulated by Dpp only during the larval stage of development (L3 only), those regulated by Dpp only during the pupal stage of development (24 only), those regulated by Dpp at both stages of development (L3/24), and those inversely regulated at the two developmental stages (inverse). A black bar represents the inverse group of genes within the L3/24 column. Magenta and green indicate up- and down-regulation, respectively.

data files and confirmed that quality data were indeed generated for this latter group of genes.

Mad-dependent regulation of Dpp targets occurs through at least two different paradigms. Dpp target genes are transcriptionally activated when Mad/Medea complexes bind "activator elements" (AEs) (Weiss et al., 2010), whereas Dpp target genes are repressed when Mad/Medea/Schnurri (Shn) complexes bind "silencer elements" (SEs) (Pyrowolakis et al., 2004). The Dpp targets changed in our experiment contain known AEs, SEs, or a mixture of both, as do the direct target genes that remained unchanged. This suggests there may be some unappreciated context-specific differences in the kinetics of the responses of SEs and AEs to Dpp signaling, which is only revealed upon short time points of induction. We also noted that *shn* was upregulated by Dpp signaling in the pupal wing (Table 1, Fig. 3), suggesting that a feedback loop incorporating new transcription of *shn* could alter the kinetics of AE versus SE driven outputs when Dpp signaling is hyperactivated.

TABLE 1. Selected Transcripts Altered by Dpp Signaling

Gene	Function/pathway	Fold change	Reference (PMID)
	24 hr APF specific		
CG15635	—	−7.06	
CG8483	Cysteine-rich secretory protein	−3.48	
p38c	MAPK signaling	−3.38	
CG34398	EGFR target gene	−2.85	22595244
kni	Target of BMP signaling pathway (repressed)	−1.59	20010841
lbk	Regulation of BMP signaling pathway	−1.58	20502686
drl	Atypical Wg receptor	−1.48	17507403
Wnt2	Wg family ligand	−1.40	
shn	Regulation of BMP signaling pathway	1.69	
ltl	Regulation of BMP signaling pathway	1.80	21266407
Ote	Regulation of BMP signaling pathway	1.85	18410727
bnl	FGF/MAPK signaling	2.16	
Dad	Regulation of BMP signaling pathway	2.65	
cv-2	Regulation of BMP signaling pathway	2.89	
spn-E	DEAD box helicase	3.15	
Trim9	Tripartite motif containing 9/interacts with Brk	3.24	14605208
hh	Hedgehog ligand	3.66	
cln3	Involved in wing vein patterning	5.68	21372148
CG9822	Cysteine-rich secretory protein	10.43	
	L3 specific		
Ac76E	cAMP biosynthetic process	−2.79	
CG14122	Pyridoxal 5′-phosphate (PLP) phosphatase	−2.55	
stumps	FGF/MAPK signaling	−1.79	15848387
pnt	ETS transcription factor, mediates EGF/MAPK	1.61	
dHig1	Hypoxia induced protein, domain	1.86	23459416
Con	Homophilic cell adhesion	2	
Pka-C3	cAMP-dependent protein kinase activity	2.10	
	L3 and 24		
Trx-2	Disulfide oxidoreductase activity	−20.55	
Rootletin	Cilia/centrosome biogenesis	−16.53	16203858
AcCoAS	Acetyl Coenzyme A synthase	−5.46	
sca	Notch signaling	−2.77	11214322
frizzled	Wingless receptor	−1.88	
easter	Protease activator of Toll signaling	2.22	
Klp54D	Microtubule-based movement	23.0	
Cyp4p1	Cytochrome P450, E-class, group I	31.0	
	Inversely regulated	**Fold difference**	
CG30288	Serine-type endopeptidase activity	31.6	
link	Target of transcription factor Zelda	7.36	22537497
IM14	Defense response/likely Toll signaling target	4	9736738
hui	Hedgehog signaling target	2.83	23749451

One outstanding question is why we see effects on known Dpp targets at the pupal stage of development, but not in the larval wing disc, where most of these targets were originally identified. We do not have a satisfactory explanation for this, but suspect that this could reflect differences in the relative strength of Dpp signaling at these two time points. During the larval stage, negative feedback loops impinge on Dpp signaling to create a precise gradient of Mad activity, a process critical for regulating overall tissue growth (Wartlick et al., 2011b). These feedback loops may be less effective, or dismantled in pupal wing tissue, where Dpp acts locally to specify wing veins (Conley et al., 2000). Thus, by expressing Tkv^{Q235D} for only 10 hr, Dpp signaling thresholds for regulating certain direct target genes may not have been attained in the larval wing disc.

To ensure that these genes were not missed in the larval disc simply due to high levels of endogenous expression in the L3 controls (thereby masking mild up-regulation during L3 in response to Dpp signaling), we compared the endogenous expression levels of the known direct Dpp target genes between the larval and pupal controls, without Dpp-signaling manipulation. We observed no differences greater than 1.2-fold in expression of these genes at the timepoints examined, except for *ltl* and *cv-2* which are 3.2-fold and 1.7-fold *lower* in the control L3 wings than the pupa. Thus the 24-hr-specific response to Dpp-signaling for these genes is not due to higher levels of endogenous expression at L3. We propose instead that our short-term induction of Dpp-signaling (10 hr) emphasizes an initial response to Dpp-signaling, while most known targets are results of a longer-term

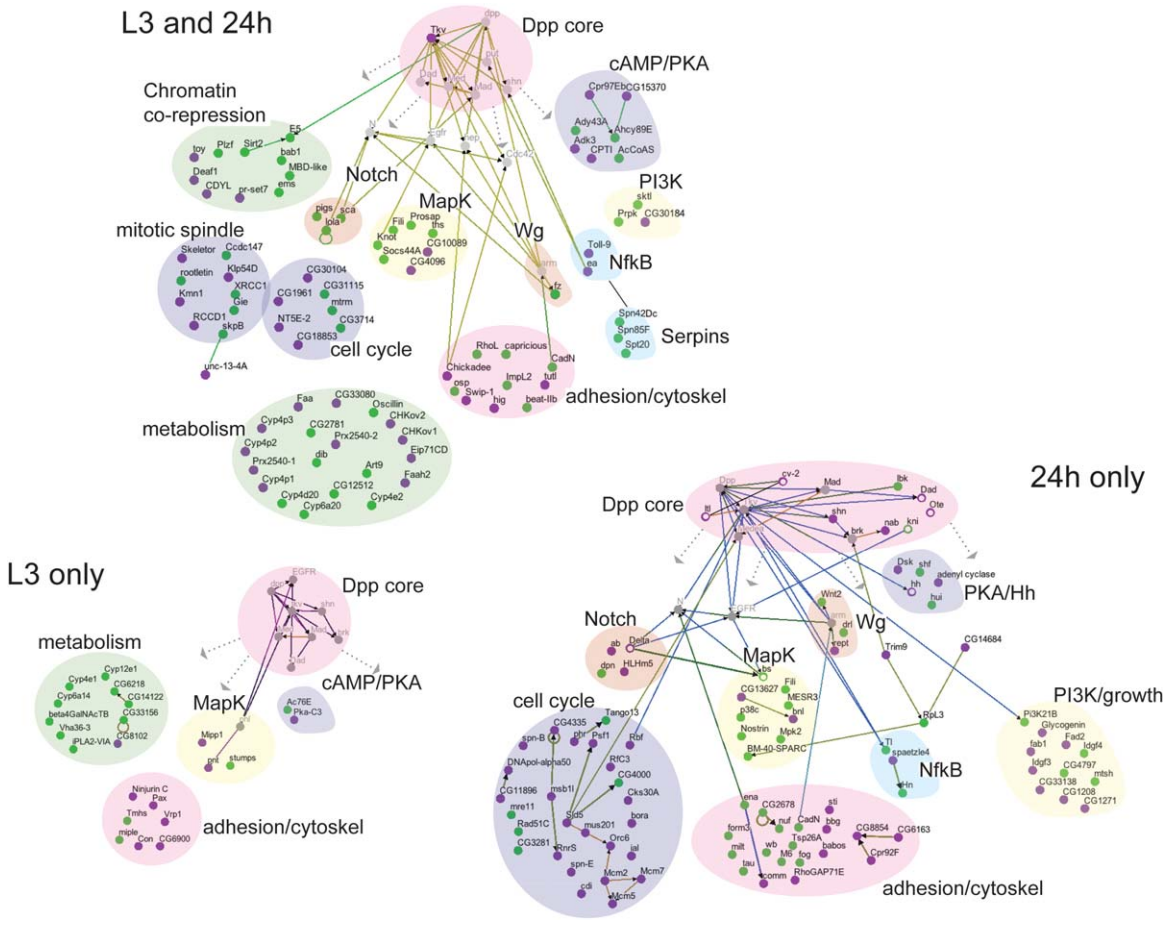

Fig. 3. Interaction networks associated with different subsets of potential Dpp targets. All nodes (except for grey nodes) were significantly affected upon Tkv activation for 10 hr (>1.3-fold, adj. $P < 0.05$ for four replicates) compared to GFP only controls at the indicated time points. Magenta and green nodes represent increased and decreased levels of expression, respectively. Grey nodes represent critical signaling interactors. Solid edges represent interactions culled from published literature and the *Drosophila* BioGRID database. Dashed arrows indicate our observed transcriptional interactions. Genes were grouped based on published functional evidence, association with a complex, or homology to known genes. Open circles indicate known Dpp transcriptional targets. Genes with multiple differentially regulated spliceforms may appear more than once.

"sustained" phase of Dpp-signaling in the larva stage. We suggest our approach may also potentially reveal stage-specific differences in the kinetics of Dpp signaling responses.

Network Analysis of Potential Dpp Targets

We next examined functional characteristics of the "L3 only," "24 only," and "L3 and 24" groups of potential target genes. We included in this analysis genes that were up- or down-regulated >1.3-fold (Table 1), known to form functional complexes with one another, or genes that genetically interact with one another (according to the BioGRID interaction database (http://thebiogrid.org) and literature searches). These data were compiled into a gene-network diagram using the network visualization program Osprey (Fig. 3). This analysis revealed several groups of interacting genes that were regulated by Dpp signaling at these developmental time points.

Genes affected by Dpp signaling at both the L3 and 24 hr APF time points were involved in signaling pathways, metabolism, the cell cycle, cell adhesion, and the regulation of transcription (Fig. 3). However, no gene ontology (GO) terms were significantly enriched in this group of genes. Dpp signaling down-regulated specific targets of Notch signaling, components of the mitogen-activated protein kinase (MAPK) signaling pathway, and the Wingless receptor *frizzled* (*fz*). In contrast, two components of the Toll (an NFKB homolog) signaling pathway were up-regulated. A group of Serpins (as well as several other serine protease inhibitors) were also down-regulated in this group. This may be significant, as Serpins have been reported to antagonize Toll signaling (Levashina et al., 1999; Reichhart, 2005).

For the "24 only" group, genes involved in several signaling pathways, including the ligand-encoding genes *delta, hedgehog, spatzle4*, and *branchless* were up-regulated. Components of the Wingless signaling pathway, however, were down-regulated (Table 2). GO terms including positive regulation of cell cycle, ectoderm development, and cell projection morphogenesis were enriched in potential pupal-specific Dpp targets (Table 2).

The network associated with the "L3 only" group of target genes was much smaller than for the "24 only" and "L3 and 24" groups. This is due to both the smaller number of "L3 only" genes found, as well as the lack of functional annotations and known

TABLE 2. GO Enrichment for Transcripts Altered by Dpp Signaling

GO Term	Enrichment *P* value
24 hr APF specific	
Wnt signaling	2.51^{-4}
Cell projection morphogenesis	1.79^{-4}
DNA helicase activity	2.8^{-6}
DNA pre-replicative complex	7.08^{-4}
Positive regulation of cell cycle	1.19^{-4}
Ectoderm development	5.82^{-4}
L3 specific	
Antioxidant activity	1.12–4

interactions for most genes in this group. A number of "L3-only" genes were involved in metabolism and the regulation of cell adhesion/cytoskeleton. Smaller groups of genes impacted Map Kinase and Protein Kinase A signaling (Fig. 3; Table 1). No GO terms were significantly enriched in down-regulated "L3 only" genes, whereas the GO term antioxidant activity was enriched ($P < 1.12^{-4}$) in up-regulated "L3 only" genes (Table 2). Altogether this network analysis suggests that Dpp-signaling outputs in the wing do not perform a discreet, simple switch from an "L3 program" to a "pupal program." Rather there is a large shared program modulated by an additional pupal program engaged during metamorphosis.

Cell-Cycle Genes Appear Up-regulated in the Pupal Wing in Response to Dpp Signaling

At 24 hr APF, wing cells have normally exited the cell cycle, and as such, no mitotic PH3- or S-phase BrdU-positive cells are observed (Schubiger and Palka, 1987; Milan et al., 1996). Tkv^{Q235D} expression from 14–24 hr APF does not induce ectopic PH3 or BrdU (Buttitta et al., 2007), and does not delay cell cycle exit in the pupal-wing epithelium (Buttitta et al., 2007). Despite this, our microarray analysis indicated that many genes involved in the cell cycle were significantly up-regulated in response to Dpp signaling in the pupal wing (Table 2, Fig. 3). There was also significant overlap ($P = 3.3^{-15}$) between the "24 only" set of potential Dpp targets, and genes we previously characterized as targets of the E2F transcription factor (Buttitta et al., 2010), a master regulator of the cell cycle (van den Heuvel and Dyson, 2008). In addition, upstream regulatory sequences associated with pupal Dpp targets were significantly enriched in binding sites for E2F (Fig. 4G). This overlap in Dpp and E2F target genes is also consistent with our previous observation that Mad and E2F binding sites are enriched upstream of cell cycle genes that share a temporal pattern of expression during wing metamorphosis (O'Keefe et al., 2012).

One pupal-specific target of Dpp signaling was Rbf (Fig. 5C), which is a negative regulator of cell-cycle progression (Du et al., 1996), and is critical for proper cell cycle exit during *Drosophila* metamorphosis (Buttitta et al., 2007). Thus, while Dpp may have up-regulated E2F target genes in the pupal wing, it also up-regulated factors that promote cell-cycle exit. To ask whether Rbf is necessary to inhibit Dpp-mediated cell cycling during pupal stages, we expressed Tkv^{Q235D} in clones of cells that lacked Rbf. In the absence of Rbf, Dpp signaling did not drive additional cell proliferation in pupal-wing tissue (data not shown). Redundant mechanisms must exist, therefore, to ensure that Dpp signaling does not drive proliferation in differentiating wing cells, despite its continued capacity to induce cell cycle gene expression.

While E2F targets were clearly affected by Dpp signaling in the pupal wing, these genes were not significantly up-regulated by Tkv^{Q235D} in the larval wing disc, where Dpp-induced proliferation is E2F dependent (Martin-Castellanos and Edgar, 2002). This is likely because E2F targets are already expressed at very high levels during the proliferative larval stages, making it difficult to detect moderate increases after a short temperature shift. In contrast, cell cycle genes are generally expressed at very low levels by 24 hr APF in the pupal wing (Buttitta et al., 2007).

To test this hypothesis, we compared the gene expression levels of our L3 only, 24-hr only, and shared L3 and 24-hr groups in the pupal wing during metamorphosis using data from O'Keefe et al. (2012) to see if our 24-hr-only group had any bias toward genes that were low in the pupal stage. We did not observe any significant bias in gene expression at any stage for the L3 only and L3+l24-hr gene groups (Fig. 4A,B). However, we did observe a slight bias for genes that decrease at 24 and 36 hr in the pupal wing for the 24-hr-only group (Fig. 4C). To discern whether this bias was caused by the presence of cell cycle genes in this cluster, which sharply decline upon cell cycle exit at 24 hr (O'Keefe et al., 2012), we parsed out the genes with cell cycle GO annotations (Fig. 4D) and reexamined the cluster without them. The removal of the cell cycle genes restored the gene expression levels for the 24-hr group to levels similar to that observed for the other groups (Fig. 4E) suggesting they primarily drive the bias we observed. This also suggests that E2F-overlapping targets are likely induced upon Dpp-signaling at *both* L3 and pupal stages, but their high expression in the proliferating controls during larval stages masked their regulation during the early timepoint. This clearly raises another potential issue with any temporal comparative analysis; while normalization of different timepoints to controls of the same timepoint will certainly introduce temporal bias (i.e., genes that change based on stage not temporal signaling), normalization of samples to the same timepoints (as we did here) can still introduce bias.

Transcription Factor Binding-Site Analysis of Putative Dpp Target Genes

To characterize the mechanisms by which target-gene specificity of the Dpp pathway is temporally regulated, we analyzed regulatory domains associated with the 624 potential Dpp targets. For these analyses, target genes were separated into four groups: (1) genes that were only regulated at the L3 time point (L3 only), (2) genes that were only regulated at the 24-hr APF time point (24 only), (3) genes that were regulated at both time points (L3 and 24), and (4) genes that were inversely regulated at the two time points (inverse). In each case, both up- and down-regulated genes were grouped together. The MEME Suite (Bailey et al., 2009) was used to identify statistically significant enrichments of known transcription factor binding sites based upon the FLYREG dataset (Halfon et al., 2008) with additional custom motifs added (O'Keefe et al., 2012). Brinker motifs and Mad/Med repressor motifs (SEs) were also curated from the literature (Pyrowolakis et al., 2004; Yao et al., 2008; Weiss et al., 2010). The search space was confined to 1 kb of sequence upstream of the transcriptional

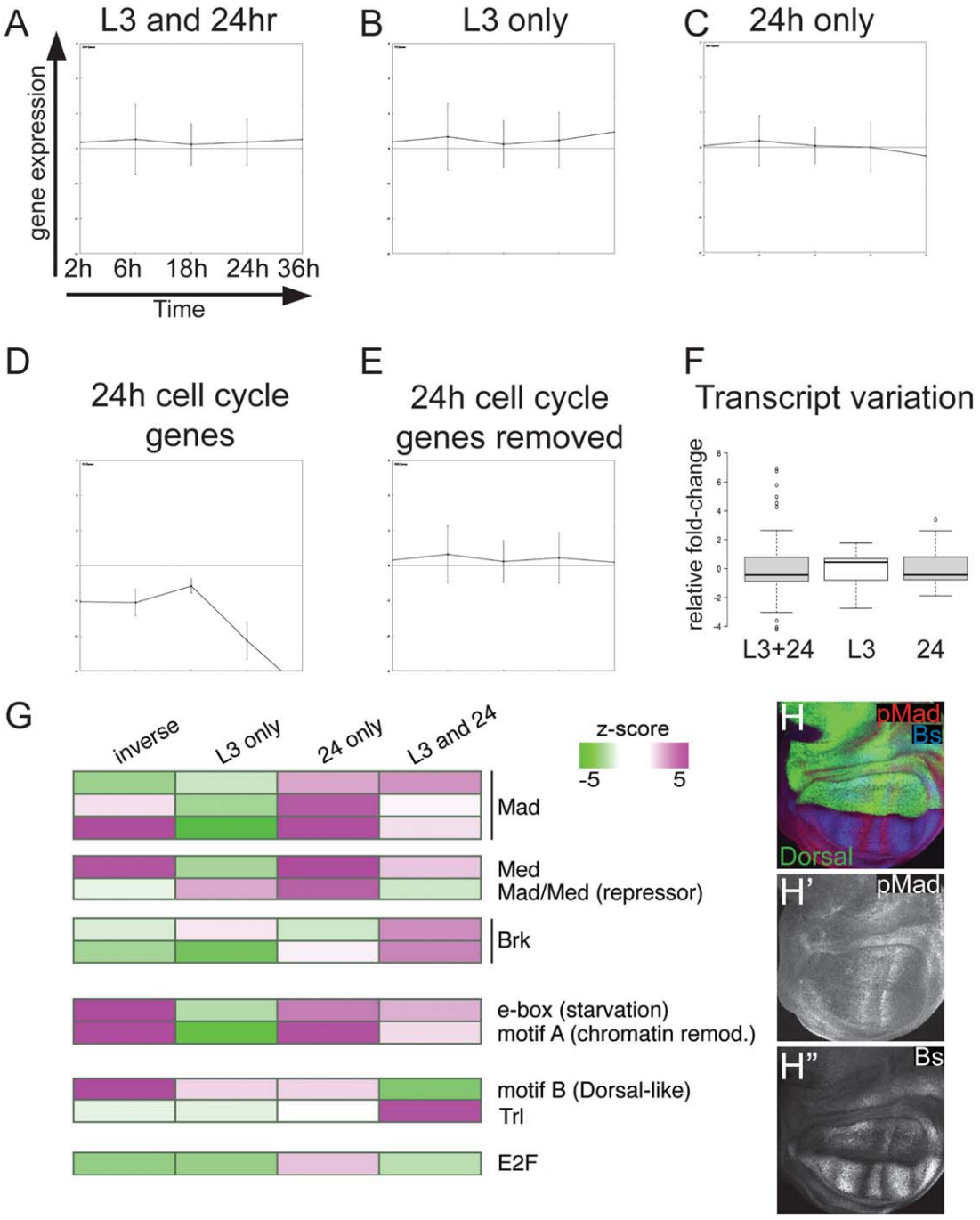

Fig. 4. Potential mechanisms by which downstream targets of Dpp signaling are temporally regulated. Average expression levels for the three indicated classes of genes altered by Dpp signaling were plotted according to their expression level over time during wing metamorphosis from L3 to 36 hr APF (data from O'Keefe et al., 2012). Transcripts in the "L3 and 24 hr" and "L3-only" groups displayed similar abundance during pupal stages (**A,B**), while an enrichment for genes that decrease during pupal stages was observed for the "24-hr-only" group (**C**). This enrichment is due to the presence of cell cycle genes in the 24-hr-only group, which decrease sharply at 24-hr APF when the wing becomes postmitotic (**D**). Removing the cell cycle genes from the 24-hr-only group restores the average expression to levels similar to the other groups (**E**). Box-plot analysis shows the relative changes in expression for each group of genes (**F**). Regulatory motif analysis of potential Dpp target genes was performed (**G**). For each group of genes, upstream sequences within 1 kb of the transcriptional start sites were analyzed via MEME to identify significantly enriched or depleted DNA motifs. Identified motifs were then compared to known motifs using TOMTOM. Z-scores from this MEME analysis are shown as a heat map, with magenta and green indicating over- and under-representation of indicated motifs, respectively. Dorsal signaling promotes vein cell fate (H). Over-expression of Dorsal in the larval wing did not affect pMad levels (i.e., Dpp signaling) (**H,H′**), but induced vein cell fate by down-regulating Bs (**H"**).

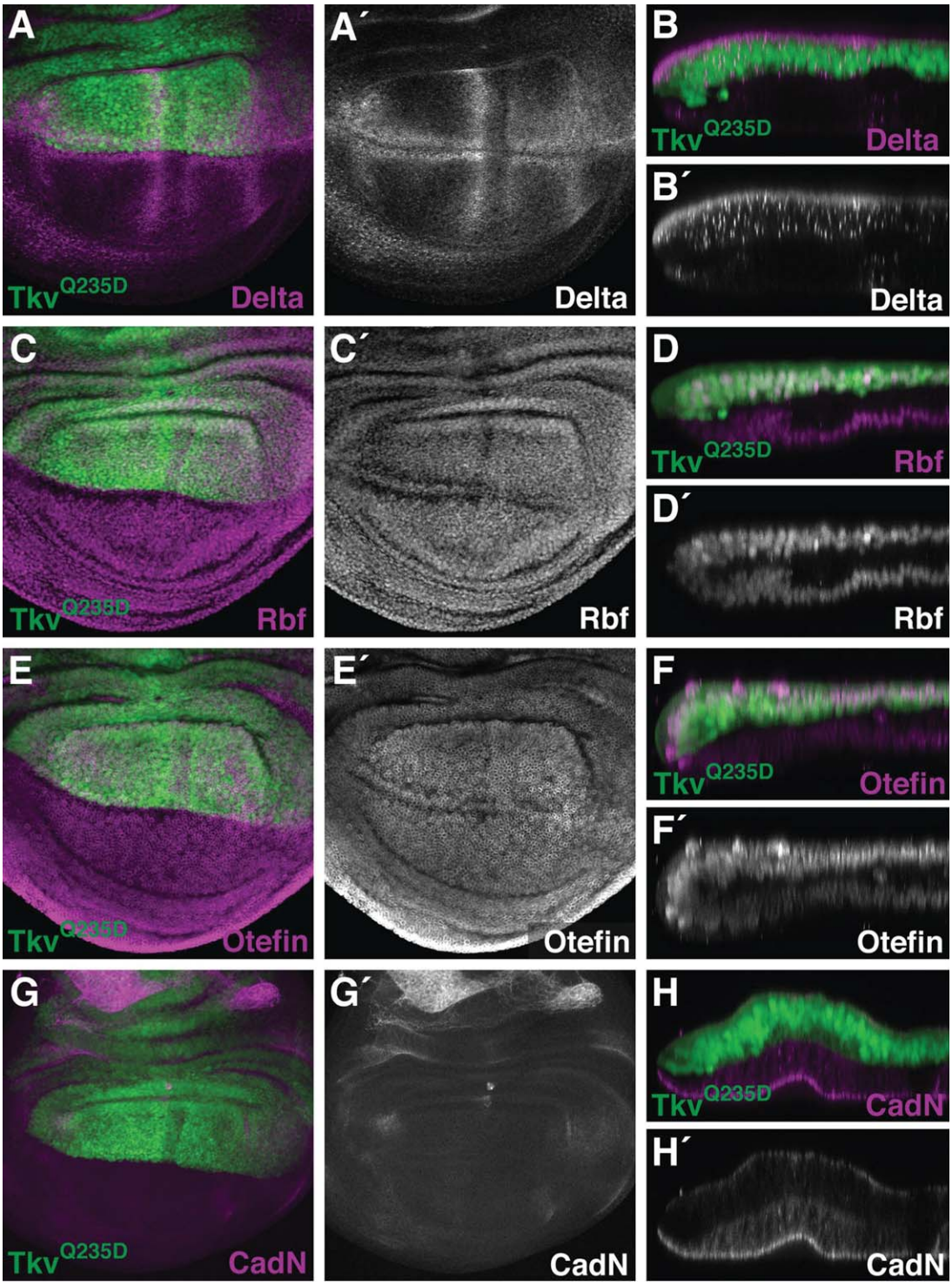

Fig. 5. Pupal-specific Dpp target genes. Using the *ap*^{ts} system, Tkv^{Q235D} was expressed in dorsal wing cells (GFP-positive) for 24 hr prior to dissection at either late L3 (**A,C,E,G**) or 24 hr APF (**B,D,F,H**). Activation of the Dpp signaling pathway had greater effects on the level of Delta, Rbf, Otefin, or CadN during pupal stages (B, D, F, H) than in the late L3 wing disc (A, B, E, G). Dpp signaling increased levels of these proteins in the pupal wing, except for CadN, which was down-regulated (H). **A′,B′,C′,D′,E′,F′,G′** and **H′** show single-channel excerpts of their respective images.

start site (see Experimental Procedures section for details) and identified motifs were then compared to known motifs using TOMTOM. Mad and Medea and Mad/Med repressor binding sites were generally enriched in these groups of target genes, with the notable exception of the "L3 only" group. This suggests that the "24 only" and "L3 and 24" groups of potential Dpp targets were transcriptionally regulated in a Mad-dependent fashion (as expected), whereas regulation of L3-specific targets may have involved other mechanisms, such as indirect effects of microRNAs or other signaling pathways.

TABLE 3. Putative Dpp target genes in the pupal wing that are also regulated by E2F

Genes	Function
Art1	Histone arginine methylation
CG10133	Phospholipase A2
CG13679	—
CG13690	RNAseH
CG14549	GINS complex helicase
CG14684	—
CG14820	Proteolysis
CG15784	—
CG17286	Spd-2 homolog, mitotic spindle
CG30377	—
CG30382	PSMA6 homolog, response to DNA damage
CG32158	Adenylate cyclase
CG3280	—
CG4069	Kelch domain containing 4 homolog
CG6854	CTP-synthase
CG6897	Bora-aurora kinase inhibitor
CG8478	Zinc binding
CG9187	GINS1 helicase homolog
Phf7	PHD finger protein 7 ortholog
chic	Cytokinesis
Cks30A	Anaphase promoting complex regulator
DNApolalpha50	DNA Polymerase
Gbp	Antimicrobial peptide production
Glycogenin	Glycogen biosynthesis
His2Av	Histone 2A variant
ial	Aurora B kinase
Mcm2	Pre-replicative complex
Mcm5	Pre-replicative complex
Mcm7	Pre-replicative complex
msb1l	—
mus201	Nucleotide excision repair
Nelf-E	RDBP homolog, mRNA binding
Orc6	Origin of replication complex assembly
Ote	Nuclear envelope assembly
phr	DNA repair
Pole2	Epsilon DNA polymerase complex
Rbf	Retinblastoma homolog
rept	RuvBL homolog, chromatin remodeling
RfC3	Replication factor C complex
RnrS	Ribonucleotide reductase
spn-B	XRCC3 homolog
spn-E	TDRD9 homolog
sti	Cytokinesis
Toll-9	Toll signaling

TABLE 4. Additional Motifs Identified Via MEME and Compared to Known Motifs With TOMTOM or Analyzed for Association With GO Term Using GOMO

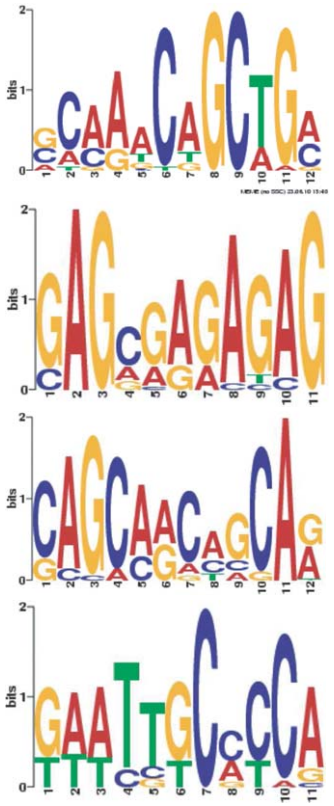

Starvation response E-box similar to Li et al. (2010)

Trl/GAGA like q = 1.9E-3

Motif A (chromatin modifier associated motif) q = 1.8E-8

Motif B (dorsal-like) q = 4.6E-1

We also identified novel motifs via unbiased searches that were similar to known motifs, or were associated with genes of particular GO terms (Fig. 4G and Table 4). These include an E-box motif similar to an E-box associated with the starvation response in larva (Li et al., 2010). This E-box motif was enriched in all groups of Dpp targets (except for L3 only) but its binding factor remains unknown. We also identified a novel motif we termed "Motif A," which was enriched in genes characterized by the GO term "chromatin modifier" (via gene ontology for motifs [GOMO] analysis). Although the significance of this motif is unknown, several chromatin modifiers were identified as putative Dpp targets in our analysis (Fig. 3).

Dpp signaling induces growth in the larval wing disc through interactions with the Hippo pathway, which acts via the transcriptional co-activator Yorkie (Yki) (Rogulja et al., 2008; Oh et al., 2013). Although Yki-associated motifs (such as the Scalloped binding site) were not enriched in our Dpp target genes, Trithorax-like (Trl) motifs, which are often associated with genes regulated by Yki (Oh et al., 2013; Bayarmagnai et al., 2012), were enriched in the "L3 and 24" shared set of genes (Fig. 4G). Using published datasets of Trl binding, we found that 65 of the 253 "L3 and 24" Dpp-target loci bind Trl in Kc cells (van Steensel et al., 2003; Negre et al., 2010). Thirteen of these genes have high-quality Trl motifs within 1 kb of their transcriptional start site, and two loci bind Trl directly (Omelina et al., 2011). The Trithorax group of genes are generally involved in maintaining gene expression as development proceeds. Loss-of-function phenotypes associated with *Trl* (e.g., small wings and loss of wing vein material), are consistent with Trl involvement in both early (proliferation) and late (wing-vein differentiation) functions of Dpp signaling (Bejarano and Busturia, 2004).

Trl has been shown to cooperate with Yki to mediate its transcriptional outputs and Yki and Trl binding on chromatin exhibits extensive overlap (Oh et al., 2013) in addition to overlap with

E2F sites (Bayarmagnai et al., 2012). Consistent with the up-regulation of cell cycle genes we observed at 24 hr in response to Dpp signaling, we also found E2F binding sites to be enriched at 24 hr (Fig. 4G). Altogether this data suggests that the growth regulatory outputs of Dpp signaling, via cooperation of Mad with Yki, Trl and E2F, occurs at both early L3 and late 24h timepoints, but Dpp-independent repression of the E2F-specific program also occurs at the pupal 24-hr stage, and even if this Dpp-independent repression is compromised, additional non-transcriptional mechanisms can compensate to restrict Dpp-induced growth and proliferation.

In contrast to the Trl motifs, Dorsal-like binding sites were enriched in the "inverse" group of Dpp targets (Fig. 4G, Table 4), with lower levels of enrichment also detected in the "L3 only" and "24 only" groups. This pattern was remarkably opposite to the Trl binding-site pattern, suggesting that Dorsal may be involved in a temporal switch in Dpp target-gene specificity rather than a common program. An interaction between these two signaling pathways is not without precedence, as inputs from both Dorsal and Dpp gradients cooperate on enhancer sites within the *ventral nervous system defective* (*vnd*) locus to generate temporal changes in *vnd* expression within the *Drosophila* embryo (Crocker and Erives, 2013). To test the hypothesis that Dorsal affects Dpp targets in the wing, we over-expressed Dorsal using the ap^{ts} system. When Dorsal was expressed during larval stages, Bs was down-regulated, but pMad levels were unaffected (Fig. 4H). As Dpp normally represses Bs only during pupal stages (Fig. 1), this suggests that Dorsal may be able to prematurely activate the late Dpp signaling program.

Confirming Pupal-Specific Dpp Targets

Most transcriptional targets of Dpp signaling in the wing have been characterized in the larval wing. Our data suggest, however, that there is an extensive pupal-specific Dpp program to be explored (Fig. 3). We, therefore, used immunohistochemistry to confirm a number of pupal-specific target genes chosen from the different gene ontology and network groups represented in Table 2 and Figure 3. These were Delta, Rbf, Otefin, and Cadherin-N (CadN). For these immunohistochemistry experiments, Tkv^{Q235D} was expressed for 24 hr before tissues were dissected at either late L3 or 24 hr APF. In each case, we confirmed that Tkv^{Q235D} expression had more dramatic effects on protein levels in the pupal wing than in the larval wing disc (Fig. 5).

Dpp Signaling Affects CadN Levels in the Pupal Wing

Inspection of pupal-specific target genes revealed novel mechanisms by which Dpp signaling affects vein-cell differentiation. For example, Dpp down-regulated CadN expression in the pupal-wing epithelium (Fig. 5H). This is consistent with low levels of CadN that we observed in wild-type vein cells (Fig. 6A,B). As cadherins mediate homophilic cell-cell adhesion (Nose et al., 1988), this suggests that vein and intervein cells may have different adhesive properties. We have previously demonstrated that vein cells express high levels of DE-cadherin (DE-cad), which is encoded by the gene, *shotgun* (O'Keefe et al., 2007). As such, reciprocal patterns of cadherin expression are seen in the pupal wing, where vein cells express high levels of DE-cad, and adjacent intervein cells express high levels of CadN (Fig. 6A,B). Reciprocal patterns of CadN and DE-cad localization have been described in other developmental contexts as well (e.g., *Drosophila* photoreceptors (Mirkovic and Mlodzik, 2006), and vertebrate neurulation (Nandadasa et al., 2009).

Signaling through both the Epidermal growth factor receptor (Egfr) and Dpp pathways specify vein cell fate. High levels of Egfr signaling are first detected in presumptive vein cells during larval stages (Sturtevant et al., 1993), whereas Dpp acts downstream of Egfr to maintain vein identity during pupal stages (de Celis, 1997). We have previously demonstrated that Egfr signaling up-regulates DE-cad levels in vein precursors, and that this process is independent of Dpp signaling (O'Keefe et al., 2007). To determine which pathway regulates CadN, we inhibited Egfr signaling (via a *UAS-Egfr-IR* transgene) in Tkv^{Q235D}-expressing pupal-wing cells and stained for CadN (Fig. 6F). We also performed the reciprocal experiment, inhibiting Dpp signaling (via Daughters against dpp (Dad)) while activating Egfr signaling (via an activated version of Ras [Ras^{V12}]) (Fig. 6E). Both experiments demonstrated that Dpp signaling regulates CadN in an Egfr-independent fashion.

Dpp Signaling Affects the Extracellular Matrix During Pupal Stages

The Dpp signaling pathway affected components of the extracellular matrix (ECM) in the pupal wing. The pupal wing blade is a bi-layered epithelial structure, with dorsal and ventral epithelia apposed at their basal surfaces. As such, components of the ECM (and associated molecules such as integrins) are critical for adhesion between the dorsal and ventral surfaces (Brower and Jaffe, 1989; Murray et al., 1995; Dominguez-Gimenez et al., 2007). Wing veins, however, represent fluid-filled gaps (i.e., tubes) between dorsal and ventral epithelia where adhesion between the wing surfaces is disrupted.

The gene *wing blister* (*wb*) encodes a component of the Laminin 1 complex and is required for dosal/ventral apposition in the wing blade (Martin et al., 1999). Tkv^{Q235D} down-regulated *wb* expression 1.76-fold at the pupal stage of development. BM-40-SPARC is a calcium-binding protein that is generally involved in tube formation and seems to stabilize basal laminae via Collagen type IV (Martinek et al., 2008). Tkv^{Q235D} down-regulated *BM-40-SPARC* 1.73-fold. *CG4096* encodes a disintegrin and metalloproteinase with thrombospondin motifs (ADAMTS), which is inferred to localize to the ECM and was recently shown to inhibit Egfr signaling (Butchar et al., 2012). *CG4096* was up-regulated >8-fold by Tkv^{Q235D}.

Finally, Dpp signaling up-regulated *CG31915*, which, based on sequence similarity, is predicted to be involved in collagen synthesis (www.flybase.org). We examined, therefore, the effect of Dpp signaling on collagen accumulation in the pupal wing. Collagen type IV (Cg25C) accumulates at the basal membrane of the wing epithelium and during larval and early pupal stages of development all wing epithelial cells are associated with collagen. By 36 hr APF, however, Cg25C specifically accumulates within vein lumens (Murray et al., 1995) (Fig. 7A). Expression of Tkv^{Q235D} throughout the dorsal wing epithelium resulted in ectopic accumulation of Cg25C (Fig. 7B). This effect was more dramatic than seen with Ras^{V12} (Fig. 7C), suggesting that the Dpp pathway plays the dominant role in regulating collagen deposition in presumptive wing-vein tissue.

Summary

Here we described a developmentally regulated switch in target-gene specificity associated with the Dpp signaling

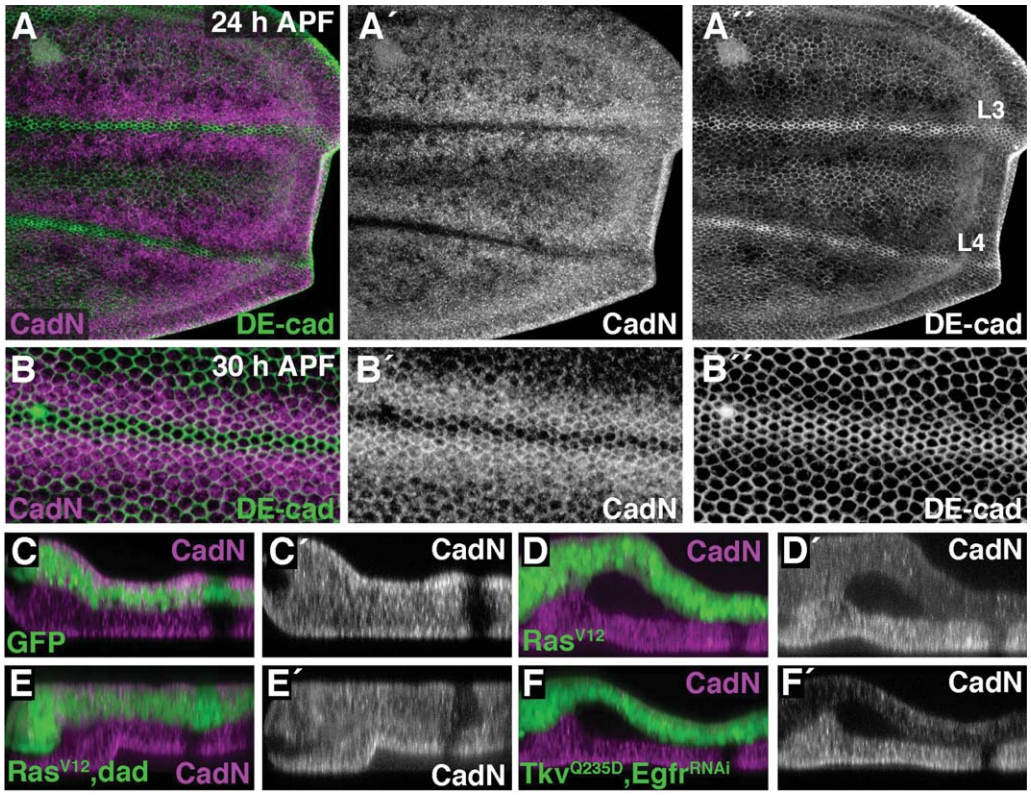

Fig. 6. Dpp down-regulates CadN in pupal-vein tissue. A,B: Wings expressing a *Ubi-DE-cad-GFP* transgene were labeled for CadN. **A:** Wing veins L3 and L4 are labeled (24 hr APF). **B:** A magnified view of vein L3 is shown (30 hr APF). DE-cad levels were highest in vein cells, whereas CadN levels were down-regulated in vein cells. **C–F:** The ap^{ts} system was used to express indicated transgenes in dorsal wing cells (GFP-positive) from 0–24-hr APF. Optical cross-sections through the posterior wing margin (left) and vein L4 are shown. Compared to the wild-type pattern of CadN localization (C), activating the Egfr/Ras signaling pathway (via an activated form of Ras [Ras^{V12}]) down-regulated CadN (D). E: Inhibiting Dpp signaling (via Dad) restored CadN levels in Ras^{V12}-expressing cells. F: Tkv^{Q235D} down-regulated CadN in the absence of Egfr signaling. **A′,A″,B′,B″, C′, D′ E′** and **F′** show the indicated single-channel excerpts of their respective images.

pathway in the *Drosophila* wing epithelium. We discovered that this is not a simple switch from a larval-specific program to a pupal-specific program. Rather there is a small larval-specific response to Dpp-signaling, overshadowed by a much larger shared response, which remains consistent between larval and pupal stages. This shared program is then combined with a pupal-specific Dpp response, which we suggest altogether encompasses the observed temporal outputs of Dpp signaling in the wing. We explored the pupa-specific program and identified specific genes that may play important roles in Dpp-induced differentiation of the wing epithelium. Finally, we identified transcription factor binding sites that were enriched in subsets of potential Dpp target genes and suggest these transcription factors may help direct the temporal outputs of the Dpp signaling pathway.

Experimental Procedures

Fly Stocks

ap^{Gal4} (Calleja et al., 1996), $tubulin\text{-}Gal80^{ts}$ (McGuire et al., 2003), $hsflp^{122}$ (Neufeld et al., 1998), $UAS\text{-}Tkv^{Q235D}$ (Nellen et al., 1996), *UAS-dorsal* (Huang et al., 2005), *Ubi-DE-cad-GFP* (Oda and Tsukita, 2001), $UAS\text{-}Ras^{V12}$ (Karim and Rubin, 1998), *UAS-Dad* (Tsuneizumi et al., 1997), *UAS-Egfr-IR* (NIG-FLY 10079R-1).

Immunohistochemistry

Wing imaginal discs and pupal wings were dissected in phosphate-buffered saline (PBS) and fixed in 4% paraformaldehyde for 20 min. Following washes in PBS-Triton (0.1%) (PBT), wings were placed in blocking solution (PBT plus 4% normal goat serum) for 2 hr at room temperature, or overnight at 4°C. Wings were incubated in primary antibody overnight at 4°C. Washes and secondary antibody incubation followed standard protocols. Primary antibodies were directed against: pMad (PS1 kindly provided by P. ten Dijke), Blistered/DSRF (Active Motif, Carlsbad, CA, 1:500), Discs large 1 (Developmental Studies Hybridoma Bank [DSHB], 1:100), Delta (DSHB, 1:100), Retinoblastoma-family protein (Rbf) (DX3 kindly provided by W. Du, 1:20), Otefin (kindly provided by D. Chen, 1:100), Cadherin-N (DSHB, 1:100), and Collagen type IV (kindly provided by J. Fessler). Other reagents included Alexa fluorescently conjugated secondary antibodies (Molecular Probes, Madison, WI; 1:1,500), and Hoechst (Life Technologies, Carlsbad, CA; 1:1,500). For pMad stainings, wings were dissected on ice. Adult wings were placed in EtOH for 1 hr, transferred to methylsalicylate for 1

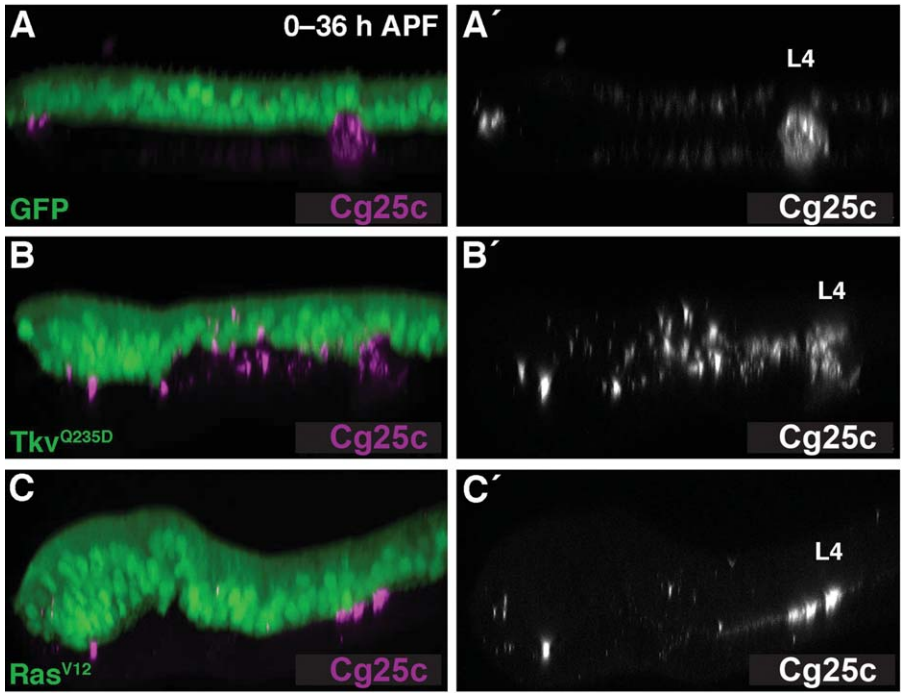

Fig. 7. Dpp promotes the deposition of extracellular matrix in the pupal wing. **A–C:** The *ap^{ts}* system was used to express indicated transgenes in dorsal wing cells (GFP-positive) from 0–24 hr APF. Optical cross sections through the posterior wing margin (left) and vein L4 are shown. Compared to the wild-type pattern of Collagen IV (Cg25C) localization (A), Tkv^{Q235D} up-regulated Cg25C throughout the wing epithelium (B). C: Ras^{V12} did not up-regulate Cg25C to the same extent as Tkv^{Q235D}. **A′, B′** and **C′** show single-channel excerpts of their respective images.

hr, and mounted in Canada balsam and methyl salicylate (1:1). Fluorescent images were acquired using a Zeiss LSM 510 confocal microscope.

Microarray Analysis

ap^{Gal4},UAS-GFP/CyO;tubulin-Gal80^{ts} flies were mated to either *hsflp^{122}*, or *hsflp^{122}; UAS-Tkv^{Q235D}*. Crosses were placed at 18°C, and larvae were raised in uncrowded conditions (less than 50 larvae per vial). For larval samples, animals were kept at 18°C until they reached the third larval instar. Vials were then transferred to 30°C. Ten hours later GFP-positive wandering larvae were collected and wing discs were dissected. For pupal samples, animals were kept at 18°C until they reached the white prepupal stage. White prepupae were then collected and allowed to develop an additional 24 hr at 18°C. Animals were then transferred to 30°C. Ten hours later GFP-positive pupae wings were dissected. Using this protocol, dissected pupal wings were developmentally equivalent to 24 hr after puparium formation (APF) (when raised entirely at 25°C). Calculations for developmental timing at 18° and 30°C were based on previously published data (as well as our own observations), which demonstrated that animals develop 2.2-fold more slowly at 18°C compared to 25°C, and 1.2-fold more quickly at 30°C compared to 25°C (Buttitta et al., 2007). Five independent biological samples were collected for each time point and each sample consisted of 10–12 wings.

RNA was extracted, amplified, and labeled as described (O'Keefe et al., 2012). Briefly, RNA was isolated from dissected tissues using Trizol (Invitrogen, Grand Island, NY), and cleaned using the RNAEasy Kit (Qiagen, Valencia, CA). For each sample, cDNA was synthesized from 500–1,000 ng of RNA. T-7-dependent linear RNA amplification was then performed using the Message Amp kit (Ambion, Life Technologies). Approximately 10 μg of amplified RNA was then labeled and hybridized to a NimbleGen expression array (Madison, WI). NimbleScan software was used to scan the arrays and for quantile normalization (all arrays were normalized together). Gene calls were generated using the Robust Multichip Average (RMA) algorithm. Statistically significant changes in gene expression were determined using ANOVA (adjusted $P < 0.05$). The data discussed in this publication have been deposited in NCBI's Gene Expression Omnibus. The GEO Series accession number is GSE39056. Network analysis of genes was visualized using Osprey (http://biodata.mshri.on.ca/osprey/servlet/Index). Centroid views of gene expression levels over time during metamorphosis (Fig. 4) were plotted using Genesis as described (O'Keefe et al., 2012).

Binding-Site Analysis

The software Find Individual Motif Occurrences (FIMO) (Bailey et al., 2006) was used (at $P < 0.0001$) to identify the locations of relevant DNA-binding motifs. Motifs are from the FLYREG dataset (Halfon et al., 2008), or custom motifs that we have described (O'Keefe et al., 2012). For all genes, FIMO scans were performed across the promoter proximal region (−1 kb to −1 bp).

To identify motifs that were enriched or depleted in given gene clusters, the sum of all motif occurrences for each cluster was calculated. Permutation tests were then performed to determine the significance of seeing that many motif occurrences at random in a cluster, as described (O'Keefe et al., 2012). A threshold z-score of |3| was chosen as significant for enrichment or depletion of motifs. Permutation tests were performed to calculate z-scores for

each cluster and motif combination. For examining co-occurrence of E2F and Tkv target genes, hypergeometric probabilities were calculated using the hypergeometric distribution (O'Keefe et al., 2012). $P < 0.05$ indicated a significant overlap. Enrichment for gene-ontology terms was examined using GORILLA (http://cbl-gorilla.cs.technion.ac.il/) with two unranked lists, where the background list included all genes present on the array ($P < 0.001$).

Acknowledgments

We thank M. Morgan, J. Davison, and the FHCRC array facility for help with microarray hybridization, processing, and data analysis. We thank the Developmental Studies Hybridoma Bank, W. Du, D. Chen, P. tenDijke, J. Curtiss, the VDRC, and the Bloomington Drosophila stock center for antibodies and stocks. This work was supported by grants from the NIH, GM070887 to B.A.E. and GM086517 to L.A.B. D.D.O. was supported by NCI 1 U54 CA132381 to the FHCRC.

References

Affolter M, Basler K. 2007. The Decapentaplegic morphogen gradient: from pattern formation to growth regulation. Nat Rev Genet 8:663–674.

Bailey TL, Williams N, Misleh C, Li WW. 2006. MEME: discovering and analyzing DNA and protein sequence motifs. Nucleic Acids Res 34:W369–373.

Bailey TL, Boden M, Buske FA, Frith M, Grant CE, Clementi L, Ren J, Li WW, Noble WS. 2009. MEME SUITE: tools for motif discovery and searching. Nucleic Acids Res 37:W202–208.

Barolo S, Posakony JW. 2002. Three habits of highly effective signaling pathways: principles of transcriptional control by developmental cell signaling. Genes Dev 16:1167–1181.

Bayarmagnai B, Nicolay BN, Islam AB, Lopez-Bigas N, Frolov MV. 2012. Drosophila GAGA factor is required for full activation of the dE2f1-Yki/Sd transcriptional program. Cell Cycle 11:4191–4202.

Bejarano F, Busturia A. 2004. Function of the Trithorax-like gene during Drosophila development. Dev Biol 268:327–341.

Brower DL, Jaffe SM. 1989. Requirement for integrins during Drosophila wing development. Nature 342:285–287.

Butchar JP, Cain D, Manivannan SN, McCue AD, Bonanno L, Halula S, Truesdell S, Austin CL, Jacobsen TL, Simcox A. 2012. New negative feedback regulators of Egfr signaling in Drosophila. Genetics 191:1213–1226.

Buttitta LA, Katzaroff AJ, Perez CL, de la Cruz A, Edgar BA. 2007. A double-assurance mechanism controls cell cycle exit upon terminal differentiation in Drosophila. Dev Cell 12:631–643.

Buttitta LA, Katzaroff AJ, Edgar BA. 2010. A robust cell cycle control mechanism limits E2F-induced proliferation of terminally differentiated cells in vivo. J Cell Biol 189:981–996.

Calleja M, Moreno E, Pelaz S, Morata G. 1996. Visualization of gene expression in living adult Drosophila. Science 274:252–255.

Conley CA, Silburn R, Singer MA, Ralston A, Rohwer-Nutter D, Olson DJ, Gelbart W, Blair SS. 2000. Crossveinless 2 contains cysteine-rich domains and is required for high levels of BMP-like activity during the formation of the cross veins in Drosophila. Development 127:3947–3959.

Crocker J, Erives A. 2013. A Schnurri/Mad/Medea complex attenuates the dorsal-twist gradient readout at vnd. Dev Biol 378:64–72.

Das P, Maduzia LL, Wang H, Finelli AL, Cho SH, Smith MM, Padgett RW. 1998. The Drosophila gene Medea demonstrates the requirement for different classes of Smads in dpp signaling. Development 125:1519–1528.

de Celis JF. 1997. Expression and function of decapentaplegic and thick veins during the differentiation of the veins in the Drosophila wing. Development 124:1007–1018.

Dominguez-Gimenez P, Brown NH, Martin-Bermudo MD. 2007. Integrin-ECM interactions regulate the changes in cell shape driving the morphogenesis of the Drosophila wing epithelium. J Cell Sci 120:1061–1071.

Du W, Vidal M, Xie JE, Dyson N. 1996. RBF, a novel RB-related gene that regulates E2F activity and interacts with cyclin E in Drosophila. Genes Dev 10:1206–1218.

Fernandez BG, Arias AM, Jacinto A. 2007. Dpp signalling orchestrates dorsal closure by regulating cell shape changes both in the amnioserosa and in the epidermis. Mech Dev 124:884–897.

Halfon MS, Gallo SM, Bergman CM. 2008. REDfly 2.0: an integrated database of cis-regulatory modules and transcription factor binding sites in Drosophila. Nucleic Acids Res 36:D594–598.

Hou XS, Goldstein ES, Perrimon N. 1997. Drosophila Jun relays the Jun amino-terminal kinase signal transduction pathway to the Decapentaplegic signal transduction pathway in regulating epithelial cell sheet movement. Genes Dev 11:1728–1737.

Huang L, Ohsako S, Tanda S. 2005. The lesswright mutation activates Rel-related proteins, leading to overproduction of larval hemocytes in *Drosophila melanogaster*. Dev Biol 280:407–420.

Inoue H, Imamura T, Ishidou Y, Takase M, Udagawa Y, Oka Y, Tsuneizumi K, Tabata T, Miyazono K, Kawabata M. 1998. Interplay of signal mediators of decapentaplegic (Dpp): molecular characterization of mothers against dpp, Medea, and daughters against dpp. Mol Biol Cell 9:2145–2156.

Irish VF, Gelbart WM. 1987. The decapentaplegic gene is required for dorsal-ventral patterning of the Drosophila embryo. Genes Dev 1:868–879.

Karim FD, Rubin GM. 1998. Ectopic expression of activated Ras1 induces hyperplastic growth and increased cell death in Drosophila imaginal tissues. Development 125:1–9.

Kim J, Johnson K, Chen HJ, Carroll S, Laughon A. 1997. Drosophila Mad binds to DNA and directly mediates activation of vestigial by Decapentaplegic. Nature 388:304–308.

Levashina EA, Langley E, Green C, Gubb D, Ashburner M, Hoffmann JA, Reichhart JM. 1999. Constitutive activation of toll-mediated antifungal defense in serpin-deficient Drosophila. Science 285:1917–1919.

Li H, Qi Y, Jasper H. 2013. Dpp signaling determines regional stem cell identity in the regenerating adult Drosophila gastrointestinal tract. Cell Rep 4:10–18.

Li L, Edgar BA, Grewal SS. 2010. Nutritional control of gene expression in Drosophila larvae via TOR, Myc and a novel cis-regulatory element. BMC Cell Biol 11:7.

Liang HL, Xu M, Chuang YC, Rushlow C. 2012. Response to the BMP gradient requires highly combinatorial inputs from multiple patterning systems in the Drosophila embryo. Development 139:1956–1964.

Lin MC, Park J, Kirov N, Rushlow C. 2006. Threshold response of C15 to the Dpp gradient in Drosophila is established by the cumulative effect of Smad and Zen activators and negative cues. Development 133:4805–4813.

Martin D, Zusman S, Li X, Williams EL, Khare N, DaRocha S, Chiquet-Ehrismann R, Baumgartner S. 1999. wing blister, a new Drosophila laminin alpha chain required for cell adhesion and migration during embryonic and imaginal development. J Cell Biol 145:191–201.

Martin-Castellanos C, Edgar BA. 2002. A characterization of the effects of Dpp signaling on cell growth and proliferation in the Drosophila wing. Development 129:1003–1013.

Martinek N, Shahab J, Saathoff M, Ringuette M. 2008. Haemocyte-derived SPARC is required for collagen-IV-dependent stability of basal laminae in Drosophila embryos. J Cell Sci 121:1671–1680.

McGuire SE, Le PT, Osborn AJ, Matsumoto K, Davis RL. 2003. Spatiotemporal rescue of memory dysfunction in Drosophila. Science 302:1765–1768.

Milan M, Campuzano S, Garcia-Bellido A. 1996. Cell cycling and patterned cell proliferation in the Drosophila wing during metamorphosis. Proc Natl Acad Sci USA 93:11687–11692.

Mirkovic I, Mlodzik M. 2006. Cooperative activities of drosophila DE-cadherin and DN-cadherin regulate the cell motility process of ommatidial rotation. Development 133:3283–3293.

Montagne J, Groppe J, Guillemin K, Krasnow MA, Gehring WJ, Affolter M. 1996. The Drosophila Serum Response Factor gene is required for the formation of intervein tissue of the wing and is allelic to blistered. Development 122:2589–2597.

Murray MA, Fessler LI, Palka J. 1995. Changing distributions of extracellular matrix components during early wing morphogenesis in Drosophila. Dev Biol 168:150–165.

Nandadasa S, Tao Q, Menon NR, Heasman J, Wylie C. 2009. N- and E-cadherins in Xenopus are specifically required in the neural and non-neural ectoderm, respectively, for F-actin assembly and morphogenetic movements. Development 136:1327–1338.

Negre N, Brown CD, Shah PK, Kheradpour P, Morrison CA, Henikoff JG, Feng X, Ahmad K, Russell S, White RA, Stein L, Henikoff S, Kellis M, White KP. 2010. A comprehensive map of insulator elements for the Drosophila genome. PLoS Genet 6: e1000814.

Nellen D, Burke R, Struhl G, Basler K. 1996. Direct and long-range action of a DPP morphogen gradient. Cell 85:357–368.

Neufeld TP, de la Cruz AF, Johnston LA, Edgar BA. 1998. Coordination of growth and cell division in the Drosophila wing. Cell 93: 1183–1193.

Nfonsam LE, Cano C, Mudge J, Schilkey FD, Curtiss J. 2012. Analysis of the transcriptomes downstream of Eyeless and the Hedgehog, Decapentaplegic and Notch signaling pathways in *Drosophila melanogaster*. PLoS One 7:e44583.

Nose A, Nagafuchi A, Takeichi M. 1988. Expressed recombinant cadherins mediate cell sorting in model systems. Cell 54:993–1001.

O'Keefe DD, Prober DA, Moyle PS, Rickoll WL, Edgar BA. 2007. Egfr/Ras signaling regulates DE-cadherin/Shotgun localization to control vein morphogenesis in the Drosophila wing. Dev Biol 311:25–39.

O'Keefe DD, Thomas SR, Bolin K, Griggs E, Edgar BA, Buttitta LA. 2012. Combinatorial control of temporal gene expression in the Drosophila wing by enhancers and core promoters. BMC Genomics 13:498.

Oda H, Tsukita S. 2001. Real-time imaging of cell-cell adherens junctions reveals that Drosophila mesoderm invagination begins with two phases of apical constriction of cells. J Cell Sci 114: 493–501.

Oh H, Irvine KD. 2011. Cooperative regulation of growth by Yorkie and Mad through bantam. Dev Cell 20:109–122.

Oh H, Slattery M, Ma L, Crofts A, White KP, Mann RS, Irvine KD. 2013. Genome-wide association of Yorkie with chromatin and chromatin-remodeling complexes. Cell Rep 3:309–318.

Omelina ES, Baricheva EM, Oshchepkov DY, Merkulova TI. 2011. Analysis and recognition of the GAGA transcription factor binding sites in Drosophila genes. Comput Biol Chem 35:363–370.

Pyrowolakis G, Hartmann B, Muller B, Basler K, Affolter M. 2004. A simple molecular complex mediates widespread BMP-induced repression during Drosophila development. Dev Cell 7:229–240.

Raisin S, Pantalacci S, Breittmayer JP, Leopold P. 2003. A new genetic locus controlling growth and proliferation in *Drosophila melanogaster*. Genetics 164:1015–1025.

Reichhart JM. 2005. Tip of another iceberg: Drosophila serpins. Trends Cell Biol 15:659–665.

Riesgo-Escovar JR, Hafen E. 1997. Drosophila Jun kinase regulates expression of decapentaplegic via the ETS-domain protein Aop and the AP-1 transcription factor DJun during dorsal closure. Genes Dev 11:1717–1727.

Rogulja D, Rauskolb C, Irvine KD. 2008. Morphogen control of wing growth through the Fat signaling pathway. Dev Cell 15:309–321.

Schubiger M, Palka J. 1987. Changing spatial patterns of DNA replication in the developing wing of Drosophila. Dev Biol 123:145–153.

Serpe M, Umulis D, Ralston A, Chen J, Olson DJ, Avanesov A, Othmer H, O'Connor MB, Blair SS. 2008. The BMP-binding protein Crossveinless 2 is a short-range, concentration-dependent, biphasic modulator of BMP signaling in Drosophila. Dev Cell 14: 940–953.

Sotillos S, de Celis JF. 2006. Regulation of decapentaplegic expression during Drosophila wing veins pupal development. Mech Dev 123:241–251.

Spencer FA, Hoffmann FM, Gelbart WM. 1982. Decapentaplegic: a gene complex affecting morphogenesis in *Drosophila melanogaster*. Cell 28:451–461.

Sturtevant MA, Roark M, Bier E. 1993. The Drosophila rhomboid gene mediates the localized formation of wing veins and interacts genetically with components of the EGF-R signaling pathway. Genes Dev 7:961–973.

Szuperak M, Salah S, Meyer EJ, Nagarajan U, Ikmi A, Gibson MC. 2011. Feedback regulation of Drosophila BMP signaling by the novel extracellular protein larval translucida. Development 138: 715–724.

Tsuneizumi K, Nakayama T, Kamoshida Y, Kornberg TB, Christian JL, Tabata T. 1997. Daughters against dpp modulates dpp organizing activity in Drosophila wing development. Nature 389: 627–631.

van den Heuvel S, Dyson NJ. 2008. Conserved functions of the pRB and E2F families. Nat Rev Mol Cell Biol 9:713–724.

van Steensel B, Delrow J, Bussemaker HJ. 2003. Genomewide analysis of Drosophila GAGA factor target genes reveals context-dependent DNA binding. Proc Natl Acad Sci USA 100: 2580–2585.

Vuilleumier R, Springhorn A, Patterson L, Koidl S, Hammerschmidt M, Affolter M, Pyrowolakis G. 2010. Control of Dpp morphogen signalling by a secreted feedback regulator. Nat Cell Biol 12:611–617.

Wartlick O, Mumcu P, Julicher F, Gonzalez-Gaitan M. 2011a. Understanding morphogenetic growth control: lessons from flies. Nat Rev Mol Cell Biol 12:594–604.

Wartlick O, Mumcu P, Kicheva A, Bittig T, Seum C, Julicher F, Gonzalez-Gaitan M. 2011b. Dynamics of Dpp signaling and proliferation control. Science 331:1154–1159.

Weiss A, Charbonnier E, Ellertsdottir E, Tsirigos A, Wolf C, Schuh R, Pyrowolakis G, Affolter M. 2010. A conserved activation element in BMP signaling during Drosophila development. Nat Struct Mol Biol 17:69–76.

Wharton SJ, Basu SP, Ashe HL. 2004. Smad affinity can direct distinct readouts of the embryonic extracellular Dpp gradient in Drosophila. Curr Biol 14:1550–1558.

Xie T, Spradling AC. 1998. decapentaplegic is essential for the maintenance and division of germline stem cells in the Drosophila ovary. Cell 94:251–260.

Yao LC, Phin S, Cho J, Rushlow C, Arora K, Warrior R. 2008. Multiple modular promoter elements drive graded brinker expression in response to the Dpp morphogen gradient. Development 135: 2183–2192.